Fuel-Cell Catalysts

DOI: 10.1002/anie.201007036

A Methanol-Tolerant Pt/$CoSe_2$ Nanobelt Cathode Catalyst for Direct Methanol Fuel Cells**

*Min-Rui Gao, Qiang Gao, Jun Jiang, Chun-Hua Cui, Wei-Tang Yao, and Shu-Hong Yu**

Direct methanol fuel cells (DMFCs) have received considerable and persistent attention, because methanol is an abundant, inexpensive liquid fuel that is easier to store and transport than hydrogen.[1] Despite the great advances made in this field, two main issues affecting efficiency and power density must still be considered, that is, sluggish kinetics of the fuel-cell anode reaction and so-called methanol crossover.[2] The small methanol molecule can easily cross over from the anode to the cathode side through the polymer membranes of DMFCs, and then reacts directly with the cathode catalyst and O_2 to decrease the cathode potential and thus reduce fuel efficiency. One approach to addressing this problem is the development of methanol-tolerant cathode catalysts for the oxygen reduction reaction (ORR). Recent research on methanol-tolerant catalysts has shown that transition metal macrocycles,[3] Ru-based chalcogenides,[4] and some platinum-based alloys[5] all show methanol tolerance while retaining catalytic activity for the ORR. Nevertheless, disadvantages still exist. For instance, Pt-free electrocatalysts often show much lower activity and inferior long-term stability under fuel-cell conditions;[6] Pt-based alloy cathode electrocatalysts are available only with low metal loading and thus are not quite suitable for DMFCs.[7] Therefore, development of novel methanol-tolerant electrocatalysts with considerable stability and high ORR activity is important.

Currently, cobalt chalcogenides are attracting enormous interest as new ORR electrocatalysts.[8] Cobalt sulfides such as Co_3S_4 and Co_9S_8 are rather active for four-electron ORR in acidic electrolytes.[9] In addition, cobalt selenides[10] and tellurides[11] show electrocatalytic ORR activity in nanocrystal form. In particular, the $CoSe_2$/C nanoparticles fabricated by Alonso-Vante et al. exhibit good methanol tolerance.[12] However, the ORR activity of these materials is still low, and they are far from DMFC application. Recently, we described a synthetic strategy that allows large-scale fabrication of ultrathin lamellar mesostructured $CoSe_2$/diethylenetriamine (DETA) nanobelts in a binary solution.[13] The lamellar nanobelts have several advantages over previous cobalt chalcogenides: homogeneously distributed, copious surface amino groups that allow loading of highly dispersed metal nanoparticles, and exceptional stability under strongly acidic conditions. With these merits, we expect that methanol-tolerant electrocatalysts with high performance can be designed on the basis of this material.

Here we report that a new methanol-tolerant Pt/$CoSe_2$ nanobelt electrocatalyst for DMFC applications can be synthesized by in situ loading of Pt nanoparticles on $CoSe_2$/DETA nanobelts through a polyol reduction approach. The Pt/$CoSe_2$ electrocatalysts display relatively high ORR catalytic activity in acidic medium. More importantly, the nanohybrid structures are highly resistant to methanol, even at concentrations of up to 5 M.

Mesostructured $CoSe_2$/DETA nanobelts were first synthesized in high yield by a simple solvothermal strategy reported previously.[13] Then, Pt NPs were synthesized in situ on the surface of $CoSe_2$/DETA nanobelts through a facile polyol reduction approach.[14] The multilayered $CoSe_2$/DETA nanobelts are highly acid resistant, although selenides are generally vulnerable to attack by acids.[15] The H_2SO_4 treatment process is followed the recent report by Kanatzidis et al. on treatment of mesostructured c-C_{20}PyPtSnSe materials with strong acids.[16] The H_2SO_4-treated sample retains the single-crystalline nature and growth direction of the original $CoSe_2$/DETA nanobelts[13] (see Supporting Information Figure S1). High-resolution (HR) TEM studies along the lateral thickness direction of H_2SO_4-treated $CoSe_2$/DETA nanobelts showed that interlayer distance decreased from 1.08 to 0.67 nm (see Supporting Information Figure S1d). In fact, acid treatment is a simple ion-exchange process.[16] Only protonated DETA molecules between two neighboring $CoSe_2$ slabs are replaced by protons, and then the flexible inorganic skeleton contracts accordingly. The results suggest that the nanobelts have exceptional stability under strongly acidic conditions and retain their shape, composition, structural integrity, and single-crystalline nature. Moreover, they have a high BET surface area of 77 $m^2 g^{-1}$ (see Supporting Information Figure S2).

Loading of Pt NPs on the surface of $CoSe_2$/DETA nanobelts was confirmed by XRD patterns (see Supporting Information Figure S3c, left). The TEM images in Figure 1a and b show that Pt NPs are homogeneously decorated on the backbone of $CoSe_2$/DETA nanobelts. The average size of the Pt NPs is about 8.3 nm (inset in Figure 1a), which corresponds

[*] Dr. M.-R. Gao, Q. Gao, J. Jiang, C.-H. Cui, W.-T. Yao, Prof. Dr. S. H. Yu
Division of Nanomaterials & Chemistry
Hefei National Laboratory for Physical Sciences at Microscale
Department of Chemistry, University of Science and Technology of China
Hefei 230026 (P. R. China)
Fax: (+86) 551-360-3040
E-mail: shyu@ustc.edu.cn
Homepage: http://staff.ustc.edu.cn/~yulab/

[**] This work was supported by the National Basic Research Program of China (2010CB934700), the National Natural Science Foundation of China (Nos. 91022032, 50732006), and the International Science & Technology Cooperation Program of China (2010DFA41170). M.R.G. thanks University of Science and Technology of China for granting Innovation Foundation of USTC for a graduate student.

Supporting information for this article is available on the WWW under http://dx.doi.org/10.1002/anie.201007036.

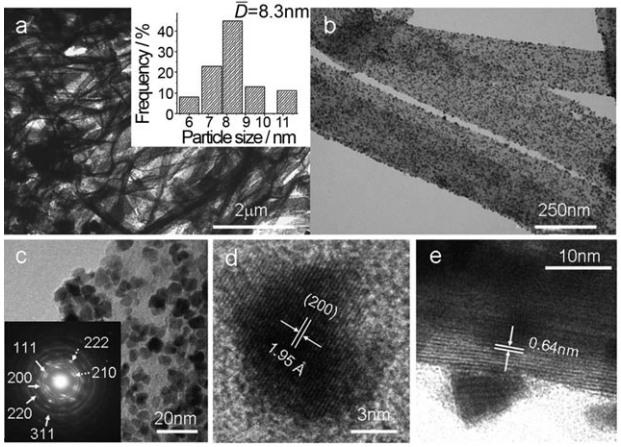

Figure 1. a–c) TEM images with different magnifications of Pt/$CoSe_2$ nanobelts prepared at 100 °C for 18 h. The inset in a) shows the corresponding particle-size histogram, and that in c) the corresponding SAED pattern. d) HRTEM image of a typical attached nanoparticle. e) HRTEM image viewed along the lateral thickness direction of a Pt/$CoSe_2$ nanobelt.

to that evaluated by using the Scherrer formula. Figure 1c clearly shows that the individual Pt NPs are well separated from each other, with no obvious aggregation of Pt NPs on the nanobelt. The selected-area electron diffraction (SAED) pattern (inset in Figure 1c) shows four intense rings indexed to (111), (200), (220), (311) planes of Pt, and also diffraction peaks of the $CoSe_2$ matrix can be detected (marked by dotted arrows). The HRTEM image in Figure 1d shows a lattice spacing of 1.95 Å, corresponding to that for the (220) facet of fcc Pt, which is consistent with the XRD result. Additionally, energy-dispersive X-ray spectroscopy (EDS) and X-ray photoelectron spectroscopy (XPS) further confirm formation of Pt on the surface of $CoSe_2$ nanobelts (see Figures S4 and S5 in the Supporting Information).

The highly ordered multilayered nanostructure of the $CoSe_2$/DETA nanobelts is well preserved after deposition of Pt NPs at 100 °C for 18 h (Figure 1e). The interlayer distance decreases from 1.08 to 0.64 nm, and two characteristic low-angle reflections of the mesostructured nanobelts become weaker, or even can not be detected (see Supporting Information, Figure S3c, right). The pH values of the starting solution before and after adding 1 mL of a solution of H_2PtCl_6 in ethylene glycol were 6.35 and 0.64, respectively. Thus, an ion-exchange process, as discussed above, occurred in the acidic medium along with the loading process, and led to uniform contraction of the interlayer distance of the $CoSe_2$/DETA nanobelts. Additionally, Pt NPs are primarily located at the two sidewalls of the nanobelts, which has the advantage of preserving the lamellar structure of the as-prepared electrocatalyst and thus allowing for higher gas permeability.

The amount of Pt NPs loaded onto the $CoSe_2$/DETA support could be effectively controlled by changing the amount of pristine $CoSe_2$/DETA nanobelts in the starting solution. An HRTEM image of Pt/$CoSe_2$/DETA nanobelts prepared in the presence of 8 mg of $CoSe_2$/DETA nanobelts in the starting solution is shown in Supporting Information Figure S6a. The loading density and size of the Pt NPs increased when 10 mg of $CoSe_2$/DETA nanobelts was used. In contrast, with 12 or 15 mg of $CoSe_2$/DETA nanobelts (see Supporting Information Figure S6b, c), the loading density and size of Pt NPs on the $CoSe_2$/DETA nanobelts decreased. The Pt NPs in all four samples are uniform in size and have homogeneous particle size distribution. The Pt loadings in the four samples, measured by inductively coupled plasma atomic-emission spectroscopy (ICP-AES) were 54.1, 39.6, 30.4, and 22.1 wt % for amounts of $CoSe_2$/DETA nanobelts of 8, 10, 12, and 15 mg (see Supporting Information Figure S6d), and are similar to typical Pt loadings of commercial Pt/C catalysts (20–60 wt %). Additionally, the shapes and facets of loaded Pt NPs can be tuned by controlling the reaction time (see Supporting Information Figure S7), which is highly desirable for specific DMFC applications owing to shape-dependent catalytic activity and durability.[3,17–19]

The attachment of the Pt NPs to the $CoSe_2$/DETA nanobelts is remarkably strong. They are not even dislodged by continuous strong ultrasonication for 2 h, even though some of the nanobelts are shattered by this treatment (see Supporting Information Figure S8a and b). This demonstrates that the Pt NPs are not simply adsorbed on the nanobelts but linked through a strong binding interaction, which may be attributed to the copious amino groups on the nanobelt surface, because amino-functionalized substrates readily and tightly couple $[PtCl_6]^{2-}$ ions.[20] To confirm the above assumption, we prepared pure $CoSe_2$ nanobelt supports without amino groups. We found that many large clusters composed of highly aggregated Pt NPs attached to the surface of these $CoSe_2$ nanobelts (see Supporting Information Figure S8c andd), which indicates a significant role of amino groups in uniform Pt dispersion.

Cobalt selenides with pyrite structure can themselves be rather active towards ORR in acidic media.[10] Figure 2a shows the polarization curves for ORR on $CoSe_2$/DETA nanobelts in N_2- and O_2-saturated 0.5 M H_2SO_4 solution at a rotating-disk electrode (RDE) at different rotation rates. In the N_2-saturated solution, no voltammetric current can be observed. In contrast, when the electrolyte solution was saturated with O_2, a catalytic reduction current began to appear and increased with increasing rotation rate due to the enhanced O_2 diffusion to the electrode surface. The ORR polarization curve of $CoSe_2$/DETA nanobelts at 1600 rpm (curve (3) in Figure 2a) shows an onset potential of up to 0.71 V versus RHE, which is similar to those reported for $CoSe_2$/C catalysts.[10a] Notably, compared with $CoSe_2$/C catalysts, the current density of $CoSe_2$/DETA nanobelts is much higher ($-1.94\ mA\,cm^{-2}$ for $CoSe_2$-DETA nanobelts and $-0.65\ mA\,cm^{-2}$ for $CoSe_2$/C at 0.3 V and 1600 rpm), although conductive materials such as carbon were not used. This result may be due to the unusual structure and high BET surface area of the $CoSe_2$/DETA nanobelts.

Figure 2b shows polarization curves for ORR on the original $CoSe_2$/DETA nanobelts, 22.1 wt % Pt/$CoSe_2$ nanobelts, and a commercial Pt/C catalyst (20 wt %, Johnson Matthey). For the Pt/$CoSe_2$ nanobelts and Pt/C catalyst, the Pt loading on the RDE was $20\ \mu g\,cm^{-2}$, whereas the $CoSe_2$ loading for pristine $CoSe_2$/DETA nanobelts was $50\ \mu g\,cm^{-2}$. In comparison to the pristine $CoSe_2$/DETA nanobelts, the

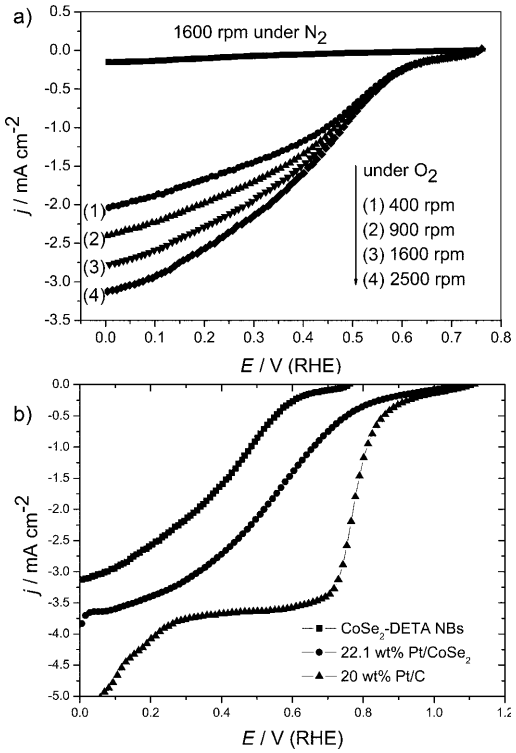

Figure 2. a) Polarization curves for ORR on pristine $CoSe_2$/DETA nanobelts in N_2. and O_2-saturated 0.5 M H_2SO_4 solutions at different rotation rates, respectively. b) Polarization curves for ORR on pristine $CoSe_2$/DETA nanobelts, 22.1 wt% Pt/$CoSe_2$ nanobelts, and 20 wt% Pt/C catalyst in O_2-saturated 0.5 M H_2SO_4 solutions at a rotation rate of 2500 rpm. Sweep rate 50 mV s^{-1}.

large positive shift in onset potential (ca. 0.3 V) revealed greatly enhanced ORR activity after decorating with Pt NPs. The onset potential of Pt/$CoSe_2$ nanobelts is the same as that of the commercial Pt/C catalyst. However, the Pt/$CoSe_2$ nanobelts exhibit broad region of mixed kinetic–diffusion control and ill-defined diffusion-limiting current, that is, they are somewhat inferior to the commercial Pt/C catalyst. We assume that the following factors could limit the performance of Pt/$CoSe_2$ nanobelts: First, the loaded Pt NPs have an average size of 8 nm, which is much larger than that of the commercial catalyst (2.5–3 nm). Second, a few aggregates consisting of several NPs are still present on the surface of the nanobelts, and limit the electrocatalytic activity of our catalyst. Third, organic species (e.g., polyvinylpyrrolidone) on the Pt surfaces may also block the active sites of the catalyst. Thus, a size-controllable and/or surfactant-free synthetic strategy is expected to further enhance the ORR property of the Pt/$CoSe_2$ catalysts.

The four-electron reduction of O_2 to H_2O has attracted a lot of attention in view of its important application in fuel cells. To evaluate O_2 reduction kinetics on Pt/$CoSe_2$ nanobelts, the 22.1 wt% Pt/$CoSe_2$ nanobelt as a typical example was investigated by rotating-disk voltammetry. A group of polarization curves for the ORR on the catalyst at different rotation rates were measured (see Supporting Information Figure S9a). High rotational speeds lead to increased O_2 diffusion to the electrode surface and large currents. The corresponding Koutecky–Levich (KL) plots (j^{-1} vs. $\omega^{-1/2}$) at various electrode potentials show good linearity and parallelism, suggesting first-order kinetics with respect to dissolved O_2 (see Supporting Information Figure S9b). Analysis of the plateau currents through KL plots reveals the reduction of O_2 with 22.1 wt% Pt/$CoSe_2$ catalyst by a four-electron process ($n = 3.8$; see Supporting Information for calculated process), which suggests nearly complete reduction of O_2 to H_2O on the new Pt/$CoSe_2$ catalysts.

Figure 3 shows that the Pt/$CoSe_2$ nanobelts have much better methanol tolerance than the commercial Pt/C catalyst. For commercial Pt/C catalyst, the ORR activity is significantly reduced in the present of methanol even at a very low concentration of 0.05 M (Figure 3a). However, the ORR onset potential and current density for Pt/$CoSe_2$ remain almost unchanged in the presence of different concentrations of methanol (Figure 3b). Remarkably, even at a very high concentration of methanol of 5 M, the reduction in ORR properties is still negligible for Pt/$CoSe_2$ nanobelts. This result is important, because it means that more fuel (methanol) can be fed at the anode, while the poisoning effect at the cathode can be ignored, and this could greatly facilitate the development of commercial DMFCs.

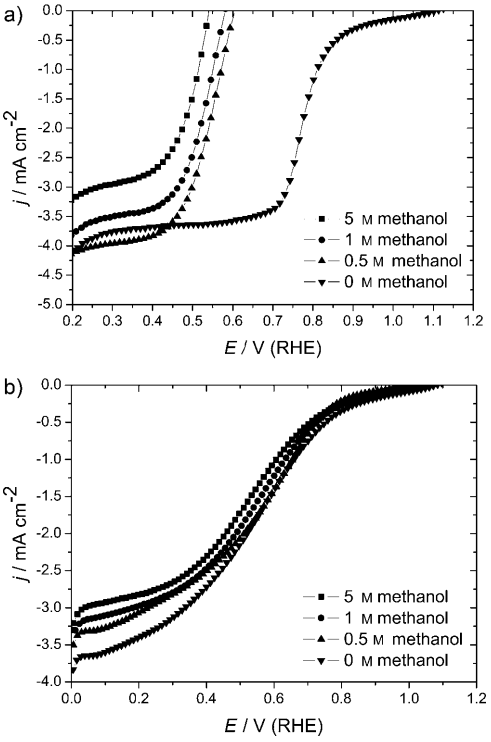

Figure 3. Polarization curves for ORR on a) 20 wt% Pt/C catalyst and b) 22.1 wt% Pt/$CoSe_2$ nanobelts in O_2-saturated 0.5 M H_2SO_4 electrolyte containing 0, 0.5, 1, and 5 M methanol at a rotation rate of 2500 rpm. Sweep rate 50 mV s^{-1}.

In summary, we have demonstrated a facile procedure to prepare nanohybrid Pt/$CoSe_2$ nanobelt electrocatalysts by a simple polyol reaction under mild chemical conditions without any molecular linkers. Pt NPs with a size of about 8 nm

can be homogeneously dispersed on $CoSe_2$/DETA nanobelts. The shape and facets of the Pt NPs on the nanobelts could be adjusted by controlling the reaction time. The Pt/$CoSe_2$ nanobelts exhibit much better ORR catalytic activity than the original $CoSe_2$/DETA nanobelts and cobalt selenides reported previously. More importantly, this new nanohybrid material with relatively high ORR activity is insensitive to methanol crossover into cathode and performs well at high methanol concentrations, which is highly desirable for cathode catalysts in DMEC and other electrochemical applications. We believe that additional improvements in the ORR activity of Pt/$CoSe_2$ may be achieved if a size-controllable and/or surfactant-free synthetic strategy can be developed.

Received: November 9, 2010
Revised: January 17, 2011
Published online: March 24, 2011

Keywords: electrochemistry · fuel cells · nanostructures · platinum · reduction

[1] a) Z. H. Wen, J. Liu, J. H. Li, *Adv. Mater.* **2008**, *20*, 743; b) M. Winter, R. J. Brodd, *Chem. Rev.* **2004**, *104*, 4245; c) G. S. Chai, I. S. Shin, J. S. Yu, *Adv. Mater.* **2004**, *16*, 2057; d) M. S. Dresselhaus, I. L. Thomas, *Nature* **2001**, *414*, 332.

[2] E. Antolini, T. Lopes, E. R. Gonzalez, *J. Alloys Compd.* **2008**, *461*, 253.

[3] a) R. Z. Jiang, D. Y. Chu, *J. Electrochem. Soc.* **2000**, *147*, 4605; b) P. Convert, C. Coutanceau, F. Claguen, C. Lamy, *J. Appl. Electrochem.* **2001**, *31*, 945.

[4] a) P. H. C. Camargo, Z. M. Peng, X. M. Lu, H. Yang, Y. N. Xia, *J. Mater. Chem.* **2009**, *19*, 1024; b) H. A. Gasteiger, S. S. Kocha, B. Sompalli, F. T. Wagner, *Appl. Catal. B* **2005**, *56*, 9.

[5] a) J. F. Drillet, A. Ee, J. Friedemann, R. Kötz, B. Schnyder, V. M. Schmidt, *Electrochim. Acta* **2002**, *47*, 1983; b) H. Yang, N. Alonso-Vante, J. M. Léger, C. Lamy, *J. Phys. Chem. B* **2004**, *108*, 1938.

[6] a) L. Xiong, A. Manthiram, *Electrochim. Acta* **2004**, *49*, 4163; b) R. C. Koffi, C. Coutanceau, E. Garnier, J. M. Léger, C. Lamy, *Electrochim. Acta* **2005**, *50*, 4117.

[7] H. Yang, C. Coutanceau, J. M. Léger, N. Alonso-Vante, C. Lamy, *J. Electroanal. Chem.* **2005**, *576*, 305.

[8] a) A. A. Gewirth, M. S. Thorum, *Inorg. Chem.* **2010**, *49*, 3557; b) Y. J. Feng, N. Alonso-Vante, *Phys. Status Solidi B* **2008**, *245*, 1792.

[9] a) Von D. Baresel, W. Sarholz, P. Schaarner, J. Schmitz, *Ber. Bunsen-Ges.* **1974**, *78*, 608; b) H. Behret, H. Binder, G. Sandstede, *Electrochim. Acta* **1975**, *20*, 111; c) R. A. Sidik, A. B. Anderson, *J. Phys. Chem. B* **2006**, *110*, 936; d) L. Zhu, D. Susac, M. Teo, K. C. Wong, P. C. Wong, R. R. Parsons, D. Bizzotto, K. A. R. Mitchell, *J. Catal.* **2008**, *258*, 235; e) Y. X. Zhou, H. B. Yao, Y. Wang, H. L. Liu, M. R. Gao, P. K. Shen, S. H. Yu, *Chem. Eur. J.* **2010**, *16*, 12000.

[10] a) Y. J. Feng, T. He, N. Alonso-Vante, *Chem. Mater.* **2008**, *20*, 26; b) E. Vayner, R. A. Sidik, A. B. Anderson, B. N. Popov, *J. Phys. Chem. C* **2007**, *111*, 10508; c) Y. J. Feng, T. He, N. Alonso-Vante, *Electrochim. Acta* **2009**, *54*, 5252; d) M. R. Gao, S. Liu, J. Jiang, C. H. Cui, W. T. Yao, S. H. Yu, *J. Mater. Chem.* **2010**, *20*, 9355.

[11] G. Wu, G. F. Cui, D. Y. Li, P. K. Shen, N. Li, *J. Mater. Chem.* **2009**, *19*, 6581.

[12] Y. J. Feng, T. He, N. Alonso-Vante, *Fuel Cells* **2010**, *10*, 77.

[13] M. R. Gao, W. T. Yao, H. B. Yao, S. H. Yu, *J. Am. Chem. Soc.* **2009**, *131*, 7486.

[14] a) J. Y. Chen, T. Herricks, M. Geissler, Y. N. Xia, *J. Am. Chem. Soc.* **2004**, *126*, 10854; b) J. Y. Chen, T. Herricks, Y. N. Xia, *Angew. Chem.* **2005**, *117*, 2645; *Angew. Chem. Int. Ed.* **2005**, *44*, 2589; c) E. Formo, E. Lee, D. Campbell, Y. N. Xia, *Nano Lett.* **2008**, *8*, 668.

[15] N. Ding, M. G. Kanatzidis, *Angew. Chem.* **2006**, *118*, 1425; *Angew. Chem. Int. Ed.* **2006**, *45*, 1397.

[16] P. N. Trikalitis, N. Ding, C. Malliakas, S. J. L. Billinge, M. G. Kanatzidis, *J. Am. Chem. Soc.* **2004**, *126*, 15326.

[17] a) N. Tian, Z. Y. Zhou, S. G. Sun, *Chem. Commun.* **2009**, 1502; b) Z. Y. Lin, H. B. Chu, Y. H. Shen, L. Wei, H. C. Liu, Y. Li, *Chem. Commun.* **2009**, 7167.

[18] L. Xiao, L. Zhuang, Y. Liu, J. T. Lu, H. D. Abruna, *J. Am. Chem. Soc.* **2009**, *131*, 602.

[19] N. Tian, Z. Y. Zhou, S. G. Sun, Y. Ding, Z. L. Wang, *Science* **2007**, *316*, 732.

[20] E. P. Lee, J. Y. Chen, Y. D. Yin, C. T. Campbell, Y. N. Xia, *Adv. Mater.* **2006**, *18*, 3271.

